TOUGHNESS - POROSITY PHENOMENA

R. E. Cooper*

INTRODUCTION

This paper reviews the evidence which shows that the fracture toughness of a material can be increased by introducing a dispersion of pores or flaws. The possible mechanisms by which this increase may be produced are then discussed and recommendations are made for further experimental and theoretical work in this field.

THE EFFECTS OF PORES ON CRACK PROPAGATION

Probably the first demonstration of the interaction of crack fronts with dispersions of fine pores was the work by Forwood and Forty [1] who produced such dispersions in single crystal sodium chloride by the diffusion of gold atoms into the lattice. When the crack front intersected a pore it propagated around it and joined up again but usually a mismatch of the cleaved surface levels occurred so that a V-shaped cleavage step resulted on the side of the pore away from the crack origin. They also observed intense dislocation generation at the crack tip while the crack was moving around the obstacle. Measurable crack retardation was observed in the pore region but no actual fracture toughness measurements were made.

Johnston et al [2] had earlier shown a porosity effect indirectly by studying the effect of unbonded alumina particles in silver chloride. At temperatures not far below the brittle ductile transition of silver chloride the work of fracture was increased. The authors considered this to be due to relaxation of triaxial stresses around the crack tip leading to a larger shear stress component and a greater amount of crack tip plastic flow.

The present author and Chapple [3] have observed similar effects in polycarbonate which contains a dispersion of spherical voids (Figure 1) and in epoxy resin containing a dispersion of PMMA spheres (Figure 2). In both these cases the characteristic V-shaped cleavage step was observed running away from the pore or inclusion on the side further from the crack origin. Fracture toughness measurements on these materials were not conclusive due to there being a large amount of scatter in the data.

The present author has determined the effects of porosity on the fracture toughness of hot pressed beryllium [4] and more recently on plasma sprayed and sintered beryllium [5]. In both materials the toughness is increased by the introduction of a small amount of porosity but the effect is more pronounced in material fabricated by the latter process. The starting powder was the same for all the five densities of material produced and they were sprayed to different densities by adjusting the spraying parameters

*Metallurgy Division, AWRE, Aldermaston, UK.

(power and stand-off distance). The sintering treatments (1400-1470°K) were slightly different for the different materials so as to produce a series of five materials with equal porosity intervals between them. Figure 3 shows a series of fracture toughness test traces (SEN specimen) and Figure 4 shows the fracture toughness as a function of porosity. It can be seen that the porosity is doubled by the introduction of 0.05 fractional porosity and that also the nature of the fracture changes from fast fracture to a controlled tearing, suggesting that the crack arrest toughness K_{Ia} is greatly increased by the porosity. Recent work by Claussen [6] (Figure 5) has shown a marked effect of zirconia inclusions on the fracture toughness of alumina. This is attributed to the presence of a fine dispersion of small cracks resulting from differential contraction of the two ceramics due to a phase change in the zirconia. The toughness increases by a factor of two on introducing 0.16 fraction of zirconia. Claussen attributed this increase to the very large number of microcracks acting as an energy absorbing crack tip zone analogous to the crack tip plastic zone in metals.

Charpy impact measurements by the present author on hot pressed beryllium show a similar although less marked effect of porosity on absorbed energy.

Some recent work on cold pressed and sintered nickel-molybdenum steels by Ingelstrom and Ustimenko [7] (Figure 6) shows that fracture toughness decreases monotonically with increasing porosity at 295 and at 200°K except for material tempered at 873°K in which when tested at 200°K there are signs of a beneficial effect of porosity just becoming detectable. The material tempered at 873°K is rather less ductile in uniaxial tension at 200°K and is probably closer to its ductile-brittle transition than is the material tempered at 923°K. Thic concept that porosity has a beneficial effect on fracture toughness only in intrinsically brittle materials or in material embrittled by being tested below their brittle-ductile transition temperature is supported by work by Ingelstrom and Nordberg on similar sintered nickel molybdenum steels [8] (Figure 7). Their measurements of fracture toughness as a function of temperature show a rapid decrease in fracture toughness below 195°K for a fully dense material but no decrease at temperatures as low as 153°K for a steel with 0.13 fractional porosity.

It would therefore appear that the introduction of some porosity increases the fracture toughness, KIC, and also increases the crack arrest toughness K_{Ia} of brittle and semi-brittle material. There is also some indication that it reduces the ductile-brittle transition temperature in sintered steels. In addition it appears that a dense array of microcracks can behave qualitatively in the same way as pores.

POSSIBLE MECHANISMS

Possible mechanisms which can be invoked to explain the phenomena reviewed above are as follows:

(i) Crack blunting by intersection of the crack front with pores;
(ii) Energy absorbtion by the pores acting as flaws leading to multiple crack paths and non-planar fracture;
(iii) Relaxation of triaxial stresses by the pores, leading to more extensive crack tip plasticity;
(iv) The porosity modifying the mechanical (tensile) properties of the material in such a way as to increase the toughness.

We can consider these in more detail as follows:

(i) Crack blunting

This is a plausible mechanism for a microstructure which can be considered to be a continuum with no features such as grain boundaries which might play a part in the fracture process. For instance a polymer such as polycarbonate or epoxy resin might be expected to exhibit toughening due to crack blunting. The author and Dr. S. R. Anthony [4] have developed a model for crack blunting and this has been described in detail elsewhere. Briefly, the problem is approached by taking the expression

$$K_{IC} = \frac{1}{2}\,\sigma_{max}\,\sqrt{\pi\rho}$$

and substituting for ρ, the crack tip radius, a composite term to include the fraction of the crack front of its natural radius d_o and the fraction of crack front which is blunted to the pore radius d. The value of σ_{max}, the maximum tensile stress at the tip of the crack, is assumed to vary with porosity in the same way as does the ultimate tensile stress.

I.e., $\sigma = \sigma_o(1 - \alpha_1\eta)$ where $\alpha_1 \sim 3.3$ for beryllium [9], and η is the fractional porosity.

The final expression obtained is

$$\frac{K_{IC(\eta)}}{K_{IC}} = \left\{ \left(\frac{d}{d_o}\right)^{1/2} \sqrt{\frac{6\eta}{\pi}} + 1 - \sqrt{\frac{6\eta}{\pi}} \right\} (1 - \alpha\eta) \qquad (1)$$

This gives fairly good agreement with experiment for the overall variation of $K_{IC(\eta)}$ with porosity. It also predicts that the larger the pores the stronger will be the effect but it has not been possible experimentally to confirm this prediction. The expression is composed of a product of two terms - the first one giving the crack blunting effect and the second one the overall decrease in K_{IC} due to the weakening effect of porosity. It thus looks functionally correct for the continuum matrix case. It does not however cover the details of the crack-pore interactions such as the formation of the V-shaped cleavage steps shown in Figures 1 and 2, bowing out of the crack between the pores, or deflection of the crack out of its plane in order to avoid pores.

(ii) Multiple flaw model

Fractography of porous beryllium [4] shows that the amount of intergranular fracture increases monotonically with increasing porosity from 5-10% in fully dense material to 100% in 0.15 fractionally porous material. This indicates clearly that the fracture process is affected by the cleavage strength of grains relative to the strength of the grain boundaries and that these relative strengths are affected by porosity. It is reasonable to assume that the cleavage strength of the grains is constant and the grain boundary strength decreases with increasing porosity due to the fabrication conditions required for less than full consolidation coinciding with those required for imperfect interparticulate bonding. Additionally the pores are all associated with grain boundaries and if pores act as stress concentrating features this will also tend to increase grain boundary fracture.

An additional observation is that the fracture surface roughness as measured at approximately a grain size or powder particle size scale increases to a maximum at 0.05-0.10 porosity and then decreases again [5].

Consider first the porosity range 0-0.1. In this range, as the amount of porosity increases the grain or interparticular boundaries become weaker and pore stress concentration effects occur so that more fracture occurs at them rather than by cleavage of grains. It is suggested that the fracture path follows the weakest set of grain boundaries and pores within the highly stressed crack tip region and there is metallographic evidence to suggest that this occurs by multiple cracking ahead of the main crack tip, these isolated "emissary" cracks then joining up to form a single fracture. For low concentrations of pores the emissary cracks will be distributed throughout a finite volume of material and the crack will deviate considerably from its nominal plane and the fracture surface roughness will increase with increasing porosity. At higher values of porosity ($\eta > 0.1$) the density of pores and emissary cracks will become so high that the main crack can propagate by linkage of them without deviating from its path and hence the fracture surface roughness will be slight.

No rigorous analysis of this model exists but some attempt can be made to quantify it as follows:

True fracture surface area

$$A = A_0 A_1(\eta) A_2(\eta)$$

where A_0 is the nominal surface area.

$A_1(\eta)$ is the normalised variation of surface area with porosity due to the presence of intersected pores on the fracture plane.

$$\therefore A_1(\eta) = 1 - \eta$$

And $A_2(\eta)$ is the normalised variation due to fracture surface topography. $A_2(\eta)$ will depend on grain boundary strength, variability of grain boundary strength, grain size, preferred orientation etc., i.e., all the factors which will be involved in determining the path which a crack will follow through a polycrystalline solid which fails partly or predominantly by intergranular fracture. No attempt will be made to obtain an expression for $A_2(\eta)$ in terms of η but one can note that for $P = 0$ $A_2(\eta) = 1$, that as $\eta \to 1$ $A_2(\eta) \to 1$ and that $A_2(\eta)$ reaches a maximum at $\eta \sim 0.07$-0.10. (η expressed as fractional porosity).

Thus we have

$$A = A_0 A_2(\eta)\ (1 - \eta)$$

Using

$$K_{IC} = \sqrt{EG}$$

we can allow for the effects of porosity by substituting from experiment [9] $E = E_0(1 - \alpha_2\eta)$ where $\alpha_2 \sim 2.4$ and $G(\eta) = G_\eta(\eta)\ \frac{A(\eta)}{A_0} = G_0(\eta)\ A_2(\eta)\ (1 - \eta)$, i.e., allowing for surface area effects.

$G_0(\eta)$ will depend on η in some indeterminate manner but an approximate estimate can be made as follows:

Since $G \simeq \sigma_y \delta$ where σ_y is yield stress and δ is the crack opening displacement it will be assumed that δ varies with porosity in the same way as does the uniaxial strain to fracture, i.e., $\varepsilon_f = \varepsilon_{fo}(1 - \alpha_3\eta)$ where $\alpha_3 \simeq 3$-4 for beryllium. The variation of σ_y is of the form

$$\sigma_y = \sigma_{y_0}(1 - \alpha_4\eta) \text{ where } \alpha_4 \simeq 2.4 \text{ for beryllium.}$$

Thus

$$G_0 = \sigma_{y_0}\varepsilon_{f_0}(1 - \alpha_3\eta)\ (1 - \alpha_4\eta)$$

and

$$G_\eta = \sigma_{y_0}\varepsilon_{f_0}(1 - \alpha_3\eta)\ (1 - \alpha_4\eta)\ (1 - \eta)A_2(\eta)$$

and therefore

$$K_{IC} = \{E_0\sigma_{y_0}\varepsilon_{f_0}(1 - \alpha_2\eta)\ (1 - \alpha_3\eta)\ (1 - \alpha_4\eta)\ (1 - \eta)A_2(\eta)\}^{1/2}$$

Normalising by dividing by

$$K_{ICO} = \{E_0\sigma_y\varepsilon_{f_0}\}^{1/2}$$

we obtain

$$\frac{K_{IC\eta}}{K_{ICO}} = \{(1 - \alpha_2\eta)\ (1 - \alpha_3\eta)\ (1 - \alpha_4\eta)\ (1 - \eta)A_2(\eta)\}^{1/2}$$

Multiplying out and ignoring higher terms in η we obtain finally

$$\frac{K_{IC}}{K_{ICO}} \simeq (1 - 4.7\eta)A_2^{1/2}(\eta) \qquad (2)$$

This expression, like the one derived for crack blunting consists of a product of a monotonically decreasing function of η which is due to the continuous decrease of mechanical properties with increasing η and a term which represents the toughening mechanism. In this case however it is not possible at present to give an analytic form for this term. It should however be possible to determine $A_2(\eta)$ experimentally in order to see whether equation (2) agrees with the experiment.

It is likely that the above model applies to many sintered metals below their ductile-brittle transition temperature and also to multiply flawed ceramics such as the Al_2O_3-ZrO_2 mentioned earlier.

(iii) Triaxial stress relaxation

In this case the term which causes the decrease in fracture toughness with increasing porosity will again be of the form (1 - const η) and be due to the decreasing mechanical properties as in 3(ii). The toughening term will be due to the crack tip material consisting effectively of many thin ligaments each in plane stress rather than being a solid block of material in plane strain. The ratio of plane stress to plane strain fracture toughness has been predicted to be 1.6 [10], suggesting a possible increase of K_{IC} with increasing porosity of about this amount. The actual form of the (K_{IC},η) curve will be given approximately by

$$K_{IC\eta} = K_c(B)\ (1 - \text{const}\ \eta)$$

where $K_c(B)$ is the fracture toughness as a function of ligament thickness, B.

A relation between B and η must be postulated and this could be done by assuming that B will be equal to the mean inter-pore distance [11].

Thus

$$B = \sqrt{\frac{\pi d^2}{6\eta}} - \frac{\pi d}{4}$$

where d is mean pore diameter.

(iv) Modification of mechanical properties by porosity

Some attempts have been made to relate fracture toughness to tensile properties by considering the processes which occur in the crack tip ligaments. Hahn and Rosenfield [10] proposed an expression

$$K_{IC} = \left\{ \frac{2}{3} E\sigma_y n^2 \varepsilon^* \right\}^{1/2}$$

where n is the strain hardening exponent and ε^* is the true tensile strain at fracture. Krafft [12] has proposed an expression $K_{IC} \propto nd_T$ where d_T is a process zone length appropriate to the crack tip plasticity and fracture processes.

There is no evidence to suggest that n increases with porosity for beryllium and all the other parameters decrease monotonically with increasing porosity so it is not possible to predict a variation of K_{IC} with η of the observed form.

CONCLUSIONS

There are now a good many examples of the toughening effect of a distribution of pores or flaws in a solid. The general reason for the effect is probably an interruption of the smooth propagation of the crack front by these microstructural features, which causes an increase in toughness, combined with a decrease in mechanical properties with increasing porosity which causes an eventual decrease in toughness at higher porosities. The exact nature of the crack front interruption process will probably depend on the type of material e.g., homogeneous polymer or sintered polycrystalline aggregate. At present three different models might be applicable and it requires further analytical development of these models together with experimental verification in order to decide which one applies to a given material.

For instance, data on the effect of pore size on toughness would help to determine the correctness of the crack blunting theory (equation (1)) quantitative surface roughness measurements would help for the multiple flaw model (equation (2)) and fracture toughness data at very small thicknesses would help for the triaxial stress relaxation model. Extensions of the experiments of Ingelstrom et al [8] to lower temperatures would show whether the sintered steels can actually show the effect found in beryllium. The models themselves require closer scrutiny and refinement, e.g., of the use of a composite term in place of the square root of the crack tip radius in the derivation of the crack blunting expression (equation (1)).

REFERENCES

1. FORWOOD, C. T. and FORTY, A. J., Phil. Mag. 11, 1965, 1067.
2. JOHNSTON, T. L., STOKES, R. J. and LI, C. H., Trans AIME 221, 1961, 792.
3. COOPER, R. E. and CHAPPLE, A., unpublished work.
4. COOPER, R. E., AWRE Report 017/72, 1972.
5. BEASLEY, D. and COOPER, R. E., to be published.
6. CLAUSSEN, N., J. Am. Ceram. Soc. 59, 1976, 49.
7. INGELSTROM, N. and USTIMENKO, V., Powder Met. 18, 1975, 303.
8. INGELSTROM, N. and NORDBERG, H., Scand. J. Met., 4, 1975, 189.
9. COOPER, R. E., ROWLAND, W. D. and BEASLEY, D., AWRE Report 025/71, 1971.
10. HAHN, G. T. and ROSENFIELD, A. R., ASTM STP 432, 1968.
11. TYSON, W., Acta Met. 11, 1963, 61.
12. KRAFFT, J. M., Appl. Mater. Res. 3, 1963, 88.

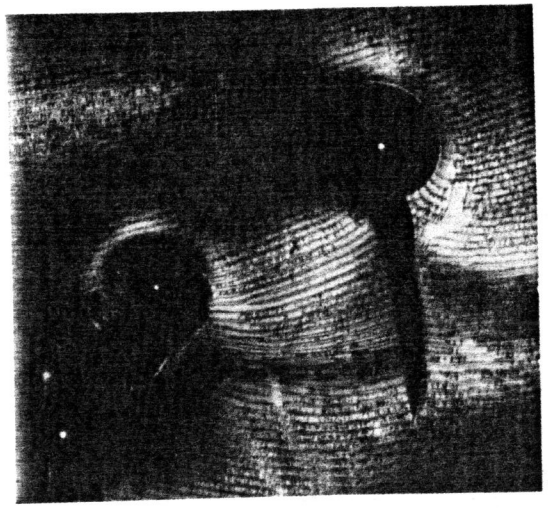

Figure 1 Optical fractograph of polycarbonate containing spherical voids approx. 120 μm diameter.

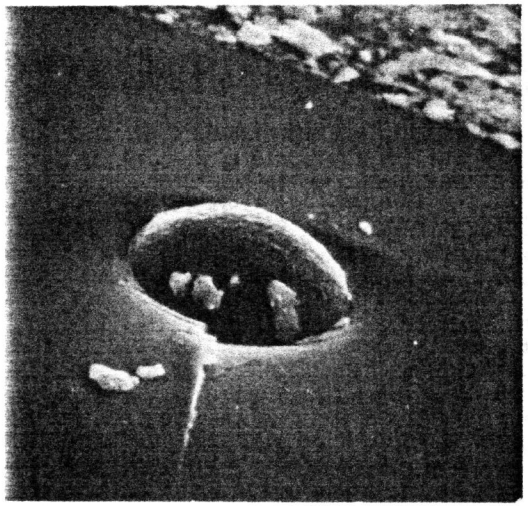

Figure 2 Scanning electron fractograph of embedded PMMA sphere 50 μm diameter in epoxy resin.

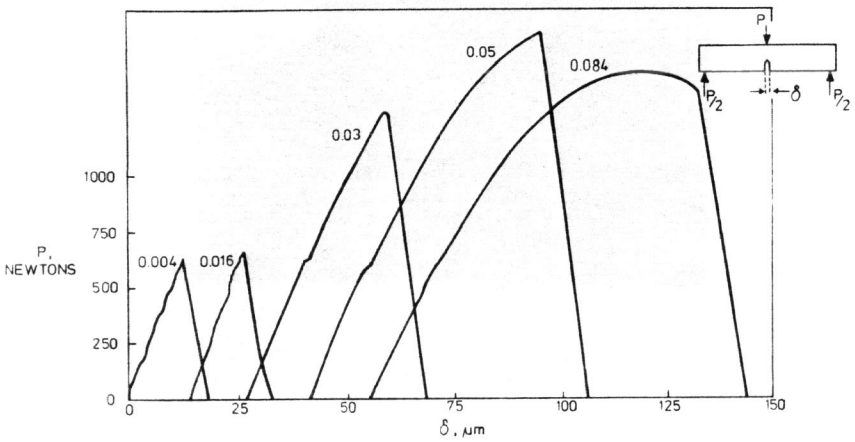

Figure 3 Fracture toughness test traces for SEN specimens of plasma sprayed and sintered beryllium. Number against each curve is the fractional porosity of the material.

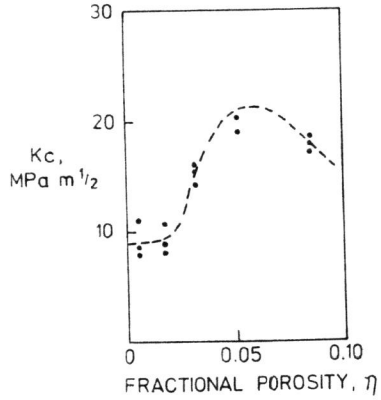

Figure 4 Fracture toughness versus porosity for plasma sprayed and sintered beryllium.

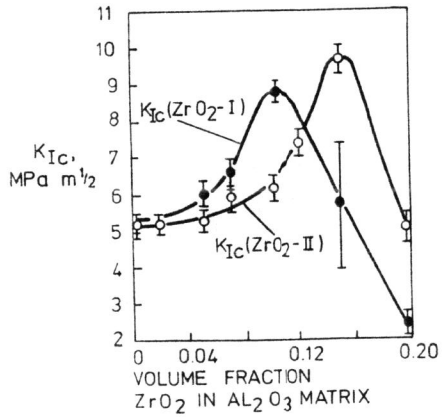

Figure 5 Fracture toughness versus inclusion content for zirconia in alumina (after Claussen).

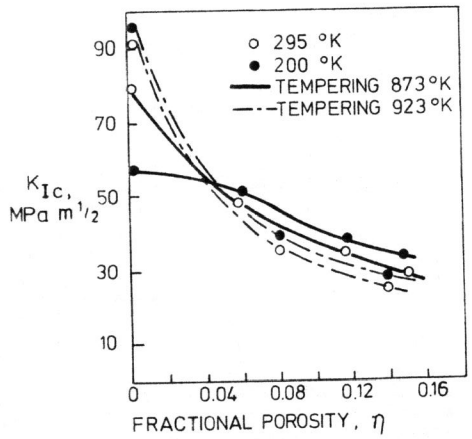

Figure 6 Fracture toughness versus porosity for sintered nickel-molybdenum steels tested at different temperatures (after Ingelstrom and Ustimenko).

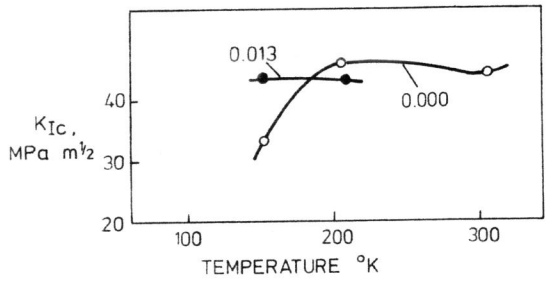

Figure 7 Fracture toughness versus temperature for sintered nickel-molybdenum steels of zero and 0.13 fractional porosities (after Ingelstrom and Nordberg).